CuZnSnSe thin film electrodes prepared by vacuum evaporation: Enhancement of surface morphology and photoelectrochemical characteristics by argon gas

Nordin Sabli[1,a], Zainal Abidin Talib[1,b], Wan Mahmood Mat Yunus[1,c], Zulkarnain Zainal[2,d], Hikmat S. Hilal[3,e], Masatoshi Fujii[4,f]

[1] Department of Physics, Faculty of Science, Universiti Putra Malaysia, 43400 UPM Serdang, Selangor, Malaysia

[2] Department of Chemistry, Faculty of Science, Universiti Putra Malaysia, 43400 UPM Serdang, Selangor, Malaysia

[3] Department of Chemistry An-Najah N.University, PO Box 7, Nablus, West Bank, Palestine

[4.] Department of Molecular Science, School of Medicine,Shimane University, Izumo, Shimane, 693-8501, Japan

[a]nordin74@gmail.com,[b]zainalat@science.upm.edu.my,[c]mahmood@science.upm.edu.my, [d]zulkar@putra.upm.edu.my, [e]hshilal@najah.edu, [f]mstfujii@med.shimane-u.ac.jp

Keywords: argon gas condensation, thermal vacuum evaporation, photoelectrochemical, CuZnSnSe, thin film

Abstract. CuZnSnSe thin films were deposited by thermal vacuum evaporation with and without argon gas stream at room temperature. Effect of argon gas on surface morphology and on photoelectrochemical (PEC) characteristics of the films was studied. The electrodes prepared under argon gas showed better enhanced characteristics, due to slower nucleation and growth due to dilution effect of the inert gas. While both electrodes showed soundly good PEC behaviors in a hexacyanoferrate(III)/hexacyanoferrate(II) redox couple, the electrode with argon gas showed 20 fold enhancement in photoactivity, compared to the one without argon gas. The results manifested thin film electrode performance can be enhanced simply by inclusion of argon inert gas inside the preparation chamber, with no need for other procedures such as annealing.

1. Introduction

The Cu_2-II-IV-VI_4 quaternary compounds Cu_2ZnSnS_4 (CZTS) and $Cu_2ZnSnSe_4$ (CZTSe) have been recognized recently as promising candidates for the next generation thin film solar cells [1,2,3]. These materials are p-type semiconductors with high absorption coefficient values ($>10^4$ cm^{-1}) and direct band gaps with optimum values (1.5 eV) for solar energy conversion. Photoelectrochemical (PEC) solar cells are being considered as replacement for traditional photovoltaiv (PV) p-n junction system [4]. Such PEC solar cells depend on the interface formed between the semiconductor and the electrolyte [5,6]. Hence, the microstructure of the semiconductor surface is of main importance [7]. Thermal evaporation of a material in the presence of argon or argon gas condensation (AGC) has many advantages over other nano-processing methods, including (i) potential deposition of many alloys with grain sizes less than 100 nm, (ii) shape similarity and narrow size distribution, and (iii) easy control of parameters [8]. Such features of the AGC method, in addition to the potential of CZTSe materials, have have attracted interest to be used in PEC systems.

Gleiter [9] used the inert gas condensation method to produce nanocrystalline powders. Since then a number of methods have been developed to prepare nanostructured thin film electrodes starting from the vapour, liquid, or solid phases [8]. Preparation of CZTSe thin films was reported using

various experimental techniques [10-12]. This work reports on the effect of argon gas on morphological and PEC characteristics of CZTSe thin films, deposited under AGC onto indium-doped tin oxide (ITO)/glass substrates. Effects of using AGC on structural, morphology, photoactivity and stability of the electrode are also discussed.

2. Experimental

2.1 Chemicals

Pottasium hexacyanoferrate (III), $K_3[Fe(CN)_6]$ and Pottasium hexacyanoferrate(II) trihydrate, $K_4[(Fe(CN)_6).H_2O$ were purchased from Sigma Aldrich. Hydrochloric acid, HCl was purchased from Friendmann Schmidt Chemical. Organic solvents, methanol and 2-propanol, were purchased from Merck KGaA and HmbG Chemicals respectively. Starting materials copper, tin, and selenium were all purchased from Alfa Aesar with nominal purity 99.8%, 99.5 and 99.5% respectively. Zinc was purchased from Nanostructured & Amorphous Materials Inc with nominal purity 99.9%.

2.2 Equipment

XRD patterns of the prepared powders and thin films were measured on a Pan Analytical XPERT-PRO X-Ray diffractometer using Cu Kα radiation [λ=1.54056Å]. Two-dimensional surface morphology was performed by using FESEM on a Nova Nano SEM 230 experiment.

2.3 Preparation of CZTSe alloys and thin film photo-electrode

The CZTSe alloy was prepared using the melt-quenching method. The mixed powder of copper, zinc, tin and selenium were weighed according to stoichiometric 2:1:1:4 nominal molar ratios, mixed, sealed in a vacuum quartz ampoule and heated. The temperature was gradually increased in a furnace from room temperature at a ramp rate of 5°C/min to reach 900°C. The furnace was continuously rocked for 48 hours to ensure proper mixing and homogeneity of the sample. The heated ampoule was then quenched rapidly in liquid nitrogen to obtain the desired alloy. The CZTSe samples were ground to powder using a mortar and a pestle. The XRD results of the CZTSe were analyzed by comparison with JCPDS Card number 98-006-7242.

The prepared CZTSe powder was then used as source material to prepare thin film electrodes using thermal evaporation method with and without AGC. The synthesized CZTSe powder (0.10 g) was placed in a molybdenum boat connected to copper electrodes inside the thermal evaporator. In order to obtain good adherence and film uniformity, the highly conductive ITO/glass substrates were pre-cleaned prior to deposition. The multi-step cleaning involved (i) washing with soap, (ii) rinsing with distilled water, (iii) washing with methanol, (iv) rinsing again with distilled water, (v) soaking in dilute HCl (10% v/v) for 10 s, (vi) rinsing with distilled water, (vii) washing with methanol, (viii) rinsing again with distilled water and (ix) drying with boiling isopropyl alcohol. The substrates were mounted on a mask 14 cm above the boat. The setup was then covered with a bell jar and evacuated to a vacuum of $5X10^{-6}$ mbar. In the absence of AGC method, the vacuum chamber pressure was maintained at 10^{-6} mbar, whereas in the AGC method the pressure was maintained at 7.5 X 10^{-4} mbar with a flow rate 5 cm^3/min. The nozzle, 0.5 mm in diameter, which flows the argon gas in, was kept adjacent to the evaporation boat pointing towards the glass substrates. Prior to deposition, the compound was pre-heated for 1 hour at a temperature lower than the compound melting point. By gradually increasing the applied current, the material in the boat turned to molten state and then evaporated. The substrates were kept at ambient temperature during the evaporation process.

2.4 The PEC experiment

PEC experiments were performed using $[Fe(CN)_6]^{-3}/[Fe(CN)_6]^{-4}$ redox couple system, by running linear sweep voltammetry between +1.0 V and -0.4 V using a PGSTAT 101 Potentiostat in a conventional three-electrode cell. A platinum counter electrode and an Ag/AgCl reference electrode

were used. A halogen lamp was used as a light source. Light intensity at the working electrode was measured to be 0.1 W/cm^2 with the aid of a pyranometer. Photo current density vs. applied potential (J-V) plots were measured under constant light intensity, whereas dark J-V plots were measured with complete exclusion of light. Electrode stability testing was performed by measuring photo current density versus time at an applied potential 0.0 V versus Ag/AgCl under illumination intensity of 0.1 W/cm^2.

3. Results and Discussion

3.1 Structural properties of synthesized powder and thin films

XRD patterns of the synthesized CZTSe powder are shown in Figure 1. XRD peaks were compared with JCPDS Card number 98-006-7242 and indexed. The XRD results confirmed the formation of polycrystalline CZTSe with the plane (112) as the strongest orientation, in agreement with earlier reports [13]. The diffraction peaks from (112), (220)/(024), (132)/(116), and (332)/(136) planes were clearly observed. The peaks well matched with the JCPDS Card.

The XRD patterns recorded for the CZTSe thin films, prepared from CZTSe powder, With-AGC and Without-AGC are shown in Figure 2. The prominent Bragg reflection occurred at or around 2θ=45° corresponding to (024) diffraction plane. A similar peak for (024) plane in CZTSe film was observed by Wei et al [14] and Z. Chen et al [15]. In Figure 2, the plane (024) peak confirms the formation of polycrystalline films in either preparation method. The results indicate a tetragonal structure, in accordance with the JCPDS Card. All structural parameters, for Without AGC and With-AGC films, are compared with the standard data (JCPDS Card number: 98-006-7242) as summarized in Table 1. The crystallite size values for the thin films, prepared at room temperature, were calculated using Scherer's formula. The average crystallite size was calculated using the prominent peak of (024) plane by using the values of full widths at half maximum (FWHM) values. The FWHM of (024) diffraction plane indicates that the crystallinity of With-AGC is higher with larger particle size compared to Without-AGC. This is presumably due to slower film growth rate in case of AGC system. Inert argon gas slows down the precipitation process, as vapor atoms coming out of the melt collide with argon atoms and lose their kinetic energy as reported earlier for other systems [16]. This would then slow down evaporation process and consequently film growth on substrate. With slower growth, higher crystallinity is expected as crystal components have more time to deposit uniformly on the formed nuclei. This explains why particle size for the With-AGC film (20.4 nm) is larger than that for the Without-AGC film (14.9 nm).

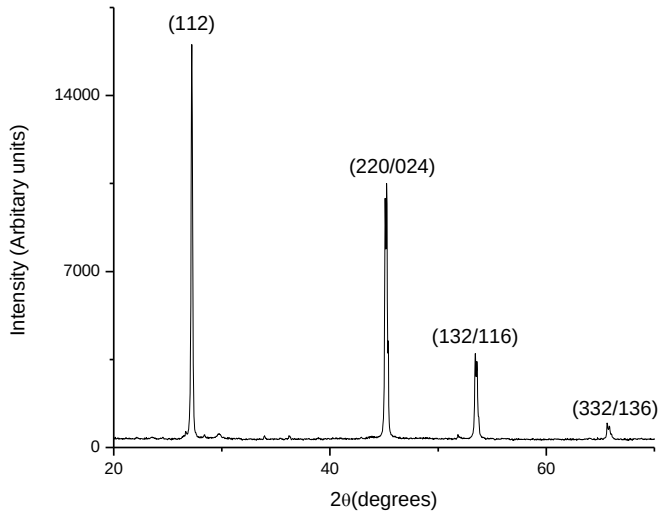

Figure 1: XRD pattern of synthesized CZTSe powder.

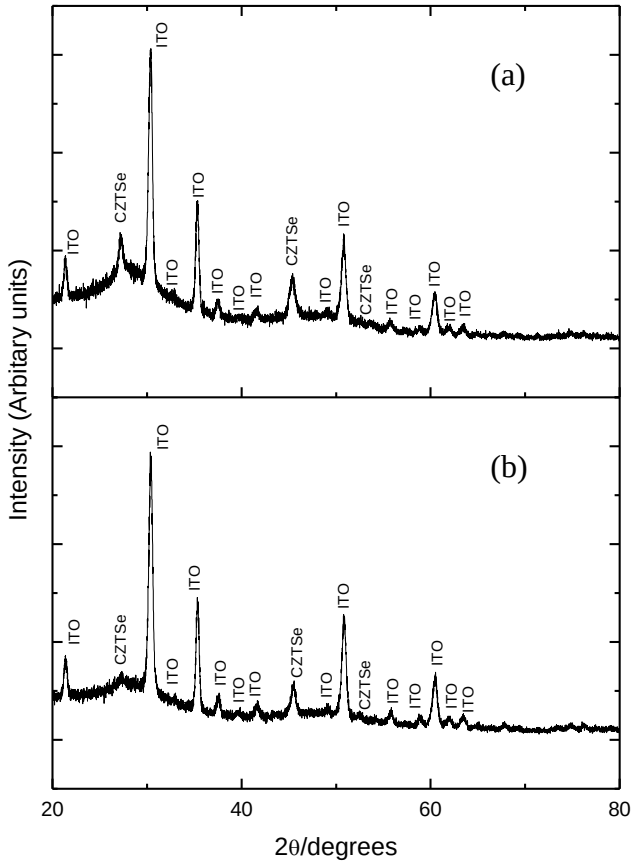

Figure 2: XRD pattern of deposited CZTSe thin films (a) Without-AGC method. (b) With-AGC method

Table 1: Comparison of various structural parameters of Without-AGC and With-AGC samples with the standard data base

Name	Angle (2θ)	Plane(*hkl*)	d(Å)	FWHM( )	Crystallite size(nm)
Without AGC	45.47	024	1.995	0.6298	14.9
With AGC	45.54	024	1.992	0.4723	20.4
JCPDS 98-006-7242	45.12	024	2.008		

3.2 Surface morphology

The surface morphology of the CZTSe thin films was studied using FESEM. Figure 3 shows the images of CZTSe thin films prepared by With- and Without-AGC. Image of the Without-AGC film shows irregularly shaped grains with sizes ranging from 40.9 to 134.0 nm. On the other hand, the With-AGC film shows well defined round shape with sizes ranging from 153.4 to 501.8 nm. The results show significant difference in morphology. Nucleation and growth condensation taking place under argon gas atmosphere are responsible for the differences in surface morphology, as discusses above. The inert argon gas slows down the precipitation process and allows more time for film components to deposit uniformly. Hence, higher crystallinity and well defined shape with larger size of particle could be observed.

3.3 Photoelectrochemical performance

A PEC cell configuration pCZTSe|Fe^{3+}, Fe^{2+}|Pt was constructed to study PEC characteristic. Different characteristics were studied including photoresponses and electrode stability. . Dark J-V plots, and photo J-V plots under 0.1 W/cm^2 intensity, are shown in Figure 4. The Figure shows positive dark currents and negative photocurrents, typical for p-type semiconductor electrodes PEC system. The negative photocurrent value continues to go negative as the applied potential goes more and more negative. This is typical behavior for p-type semiconductor working electrodes [17], and is totally consistent with earlier reports [10].

Figure 5 shows net photo J-V plots, calculated by subtracting dark J-V plots from observed photo J-V plots for With- and Without-AGC film electrodes. Higher current density values can be observed for With-AGC film. The difference between the two systems indicates enhancement in photoresponse values by using argon gas. Higher current density values and photoresponses indicate lower resistance and better charge transfer across the solid/redox couple interface, in case of the AGC system.

The stability of both electrode systems was studied by monitoring the value of photo current density under steady illumination intensity over a period of 7 hours, with zero applied potential. The results are shown in Figure 6. The With-AGC film shows that the photocurrent intensity increased at the beginning, and then showed a steady value with time. On the other hand, the Without AGC started with certain value and steadily decreased with time. Moreover, the With-AGC system showed higher short circuit current throughout the whole process, in accordance with results discussed above. The Figure indicates that inclusion of argon gas enhanced both photoresponse and stability of the thin film electrode under PEC conditions.

The enhancement in electrode PEC characteristic, by AGC method, goes in parallel with enhancement in crystallite sizes and film morphology discussed above. Moreover, the argon gas effect is in parallel with annealing effect on thin film electrodes, commonly reported in literature [18-19]. Effect of annealing on surface morphology/texture was reported for different metal chalcogenides [18-21] for the purpose of PEC efficiency improvement. The With AGC method resembles annealing effect by enhancing crystallinity and removing defects. This lowers recombination and traps inside grains and at the grain boundaries. In this present work, the photoactivity was increased by about 20 fold when using AGC method. Such photoactivity enhancement is due to enhanced electrode morphology that results from nucleation and growth mechanism of the thin film. The introduction of argon gas inside the evaporation chamber during thermal vacuum evaporation process is thus responsible for such enhancement. It is therefore recommended to use such technique in future thin film electrode preparations, as only one step preparation is needed to enhance the resulting electrodes. Investigation of the combined effects of argon gas inclusion during film preparation, followed by annealing the resulting film, is under way here.

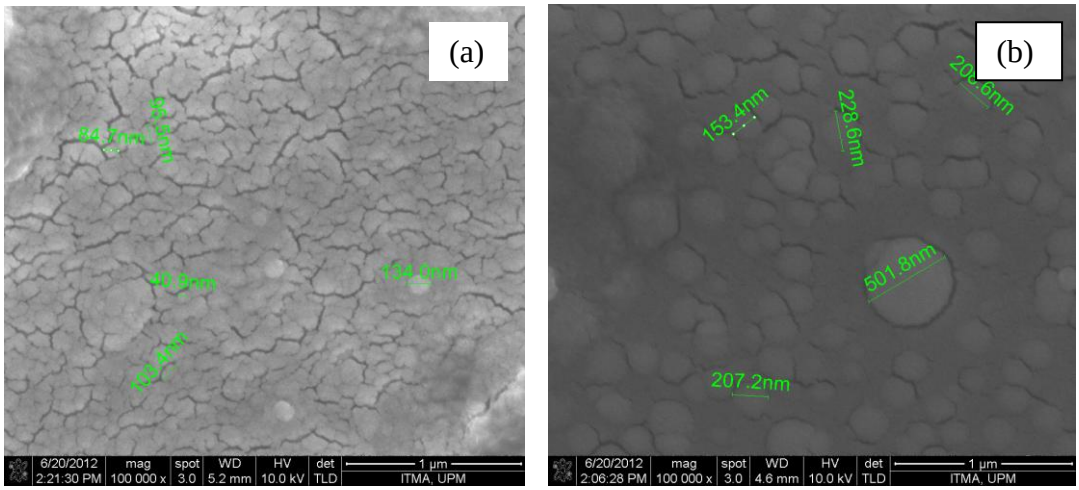

Figure 3: Two dimensional SEM images for surface morphology of (a) Without-AGC and (b) With-AGC of CZTSe thin films

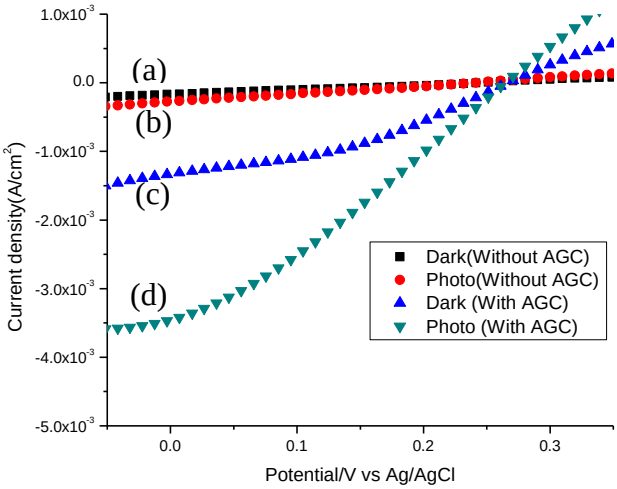

Figure 4: Effect of (a) Without-AGC dark, (b) Without-AGC photo, (c) With-AGC dark and (d) With-AGC photo thin film electrode on J-V characteristics

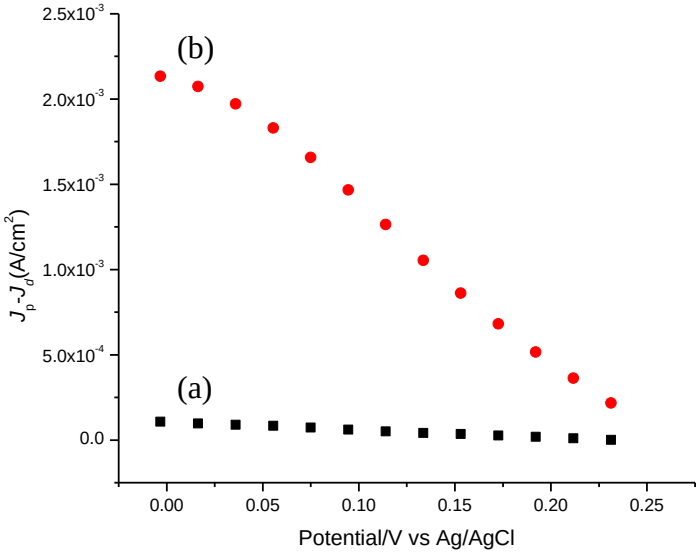

Figure 5: Difference between the photocurrent (J_p) and darkcurrent (J_d) for (a) Without-AGC and (b) With-AGC thin film electrodes

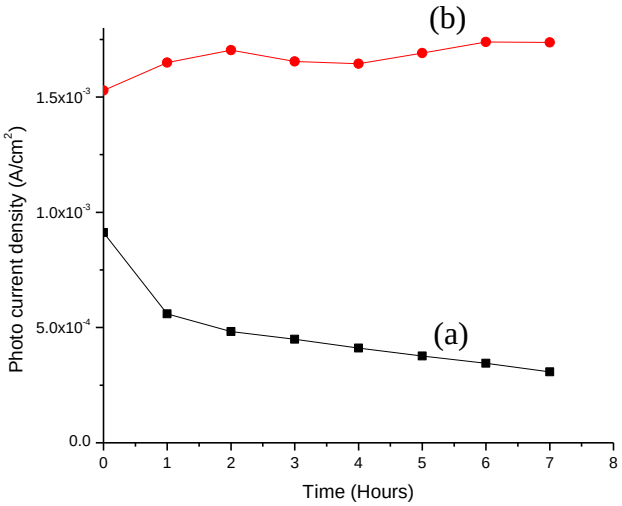

Figure 6: Short-circuit current density vs. time measured for (a) Without-AGC and (b) With-AGC thin films electrode

4. Conclusions

By introducing argon gas inside evaporation chamber, during thermal vacuum evaporation process, the characteristics of CuZnSnSe thin film were enhanced. The argon gas enhanced the surface morphology and crystallite sizes of the thin film electrode. Both photoactivity and stability of the electrode, in ferricyanide/ferrocyanide redox couple systems, were also enhanced by argon gas inclusion in the preparation. The results show the potential future value of using AGC even without annealing the electrode. Investigating the combined effects of using AGC during electrode preparation, followed by annealing, on the PEC characteristics, is worth to investigate.

Acknowledgement

The support of this research by Ministry of Higher Education of Exploratory Research Grant Scheme Grant no. 5527051 and UPM research university grant scheme is gratefully acknowledged.

References

[1] W.Haas, T.Rath, A.Pein, J.Rattenberger, G.Trimmel,F.Hofer, Chemical Communications.47 (2011) 2050-2052

[2] A.Redinger, S.Siebentritt, Appllied Physics Letters 97 (2010) 092111

[3] K.Timmo, M.Altosaar, J.audoja, K.Muska, M.Pilvet, M.Kauk, T.Varema, M.Danilson, O.Volobujeva, E.Mellikov, Solar Energy Materials & Solar Cells 94 (2010) 1889-1892

[4] M.Gratzel, Nature 414 (2001) 338-344

[5]P.P.Hankare, P.A.Chate, D.J.Sathe, M.R.Asabe, B.V.Jadhav, Solid State Sciences 10 (2008) 1970-1975

[6] O.Savadogo and K.C.Mandal, Materials Chemistry and Physics (1992) 301-309

[7]P.P.Hankare, P.A.Chate, D.J.Sathe, M.R.Asabe, B.V.Jadhav, Solid State Sciences 10 (2008) 1970-1975

[8]C.C.Koch, Nanostructured Materials:Processing, Properties and Applications, second ed., William Andrew, Inc, Norwich, NY, 2007, 47-90

[9] H.Gleiter, Progress in Material Science 33 (1989) 223-315

[10] R.A.Wibowo, W.S.Kim, E.S.Lee, B.Munir, K.H.Kim, Jounal of Physics and Chemistry of Solids 68 (2007) 1908-1913

[11] S.Bag, O.Gunawan, T.Gokmen, Y.Zhu, T.K.Todorov, D.B.Mitzi, Energy & Environmental Science 5 (2012) 7060

[12]M.Tsega, D.Kuo, Applied Physics Express 5 (2012) 091201

[13] A.Nagaoka, K.Yoshino, H.Taniguchi, T.Taniyama, H.Miyake, Journal of Crystal Growth 354-1 (2012) 147-151

[14] H.Wei, W.Guo, Y.Sun, Z.Yang, Y.Zhang, Materials Letters 6413 (2010) 1424-1426

[15] Z.Chen, L.Han, L.Wan, C.Zhang, H.Niu, J.Xu, Applied Surface Science 257-20 (2011) 8490-8492

[16] V.Hass, H.Gleiter and R.Birringer, Scripta Metallurgica et Materialia 28 (1993) 721-724

[17] H. Finklea, , Semiconductor Electrodes, Elsevier, ed., Amserdam, (1988), 393-448

[18] H.S.Hilal, R.M.A.Ismail, A.El-Hamouz, A.Zyoud, I.Saadeddin, Electrochimica Acta (2009) 3433-3440

[19] Z.Zainal, N.Saravanan, K.Anuar, M.Z.Hussein, W.M.M.Yunus, AJSTD 21-1(2004) 11-17

[20]P.P.Hankare, P.A.Chate, P.A.Chavan, D.J.Sathe, Journal of Alloys and Compounds 461 (2008) 623-627

[21] Z.Zainal, S.Nagalingam, A.Kassim.,M.Z.Hussein, W.M.M.Yunus , Solar Energy Materias & Solar Cells (2004) 261-268